



NATIONAL AERONAUTICS AND SPACE ADMINISTRATION

SCATTEROMETER DATA ANALYSIS TECHNIQUES

CRES TECHNICAL REPORT 118-3

By

H. W. Masenthin  
Remote Sensing Laboratory  
University of Kansas  
Lawrence, Kansas

July 1967



Prepared by the University of Kansas Center for Research, Inc.,  
Engineering Science Division, Lawrence, Kansas, for the National  
Aeronautics and Space Administration (NASA) under NASA  
Contract No. NSR 17-004-003 and NAS 9-7175.

N 69-15722

(ACCESSION NUMBER)

(THRU)

(CODE)

(CATEGORY)

(NASA CR OR TMX OR AD NUMBER)

MANNED SPACECRAFT CENTER  
HOUSTON, TEXAS

FACILITY FORM 602

84 254301

Technical Report  
118-3

SCATTEROMETER DATA ANALYSIS TECHNIQUES\*

by

H. W. Masenthin

July 25, 1967

The Remote Sensing Laboratory

\*The research reported on here has been sponsored by the National Aeronautics and Space Administration under contract NSR 17-004-003 and NAS 9-7175. Reproduction in whole or in part is permitted for any purpose of the United States Government.

## ABSTRACT

Radar scatterometry programs in the past have been almost entirely motivated by the need for radar design information. This emphasis has limited both the amount of ground truth information obtained and the development of data interpretation techniques. Most of the data obtained in these programs is summarized in scattering cross section versus angle of incidence curves that are identified by the radar parameters and relatively gross descriptions of the surface (New Jersey woods, Lake Michigan, city of Chicago, etc.)

This report discusses the use of scatterometry as a geoscience tool for discrimination and identification of terrain surfaces. The volume of data that must be interpreted in such an application makes it mandatory that a presentation technique be used that permits simultaneous scanning of multiple parameter data at a much faster rate than can be achieved with the normal scattering coefficient versus angle of incidence curves.

Data from Pissgah Crater, California is analyzed to determine the ability of the scatterometer to discriminate various surfaces. These data are shown in a variety of presentations that might be considered for use by geoscience investigators.

## Technical Report 118-3

Herb Masenthin

### I. Introduction

This report covers processing of data from the Ryan Scatterometer used on NASA Mission Number 21 on 5 April 1967 over Pisgah Crater in California.

A brief description of the Ryan Scatterometer system is given. Methods and problems of identifying the data are explained. The data was processed by hand to obtain certain results and will be further processed by computer programs.

Several methods of presenting the data in an easily understood method were attempted. Possibilities, problems and results are discussed.

### II. Brief Description of the Ryan Scatterometer System

The Ryan Scatterometer is described thoroughly in CRES Report No. 61-11, Ryan Report No. 57672-1 and other technical reports and will be discussed only briefly here.

The Ryan Scatterometer is a continuous wave fan beam radar as shown in Figure 1. Return data is taken continuously as the plane flies along its flight path. Due to the aircraft velocity, the radar return includes doppler frequencies, different frequencies corresponding to different angles within the fan beam and therefore to different ground areas. The return from selected areas can be separated from the total return by a series of frequency filters. For this experiment data was recorded for areas at  $\pm 5^\circ$ ,  $\pm 10^\circ$ ,  $\pm 15^\circ$ ,  $\pm 20^\circ$ ,  $\pm 30^\circ$ ,  $\pm 40^\circ$ ,  $\pm 50^\circ$ , and  $\pm 60^\circ$ . As the aircraft proceeds along the flight path the radar return from each area is recorded for each of the 16 angles. This information is stored and later processed by a computer into graphs displaying return strength vs. angle for each ground area.

The size of the ground area (resolution cell) which is examined by the radar can be calculated as follows: The length of the area (x in Figure 1)

is determined by the range of doppler frequencies selected by the frequency filters. At an angle  $\theta$  from the vertical, the doppler frequency is  $f_d = \frac{2v}{\lambda} \sin \theta$  where  $v$  is the aircraft velocity and  $\lambda$  is the wavelength of the radar transmitter. The length of the ground area can be selected by a range of doppler frequencies  $f_d = \frac{2v}{\lambda} (\sin \theta_2 - \sin \theta_1)$  where  $\theta_2$  is the angle from vertical to the far side of the area and  $\theta_1$  is the angle to the near side. Typical values of  $f_d$  range from  $4.6 v$  to  $0.6 v$  as  $\theta$  varies from  $3^\circ$  to  $60^\circ$ , to maintain a constant length  $x$  of approximately 200 feet.

The width ( $r_{az}$  in Figure 1) can be calculated approximately

by  $r_{az} = \frac{h}{\cos \theta} \sin \beta = \frac{h}{\cos \theta} \beta$  (for  $\beta$  small), where  $h$  is the vertical aircraft height and  $\beta$  is the radar beamwidth in radians. This shows  $r_{az}$  varies from  $h\beta$  at  $\theta=0^\circ$  to  $2h\beta$  at  $\theta=60^\circ$ . For this flight  $r_{az}$  would vary from approximately 175 ft. at  $\theta=0^\circ$  to 350 ft. at  $\theta=60^\circ$ . For this flight the resolution cell was selected to be square at  $\theta=30^\circ$ . The length  $x$  was maintained constant at all angles, therefore the resolution cell area varied with  $\theta$ .

### III. Data Received

The data received by CRES consisted primarily of the following:

#### A. Pisgah Crater Flight

1. Flight log book listing information about flight times, locations, altitude and equipment used,
2. Approximately 150 graphs with two Return vs. Angle plots on each, from the forebeam data.
3. A similar set of graphs for the aftbeam.
4. Aerial photographs of Pisgah Crater, taken at the same time as the scatterometry data.

#### B. Bermuda area ocean flight

1. Flight log book
2. Several thousand Return vs. Angle plots
3. Power Spectrum curves (Energy Density vs. Log Number or Period in seconds) for the sea state during the time of the flight.

#### IV. Data Processing

As the first step in processing the Pisgah Crater data, the aerial photos were mounted in sequence on boards for convenience, and were covered with a plastic overlay.

The flight line was marked across the center of each photograph, assuming the photos had been taken vertically downward from the plane. The time of each photograph was read from the edge of the photo; this time was assumed to be at the center of the photo.

The scale of the aerial photographs was determined by comparing the length of a prominent road section on the photo with the same road section on a map. The photo scale was found to be approximately 1:10,000.

After the photo scale had been determined, the beam width on the ground could be calculated by the formula  $X = r\theta$ . For this flight  $r$  (airplane height) was 4000 ft.  $\theta$  (beamwidth in degrees) was  $2.5^\circ$  and  $x$  (beamwidth on the ground directly below the aircraft) was found to be 63.5 meters or 0.635 cm to scale on the photos. The beamwidth was drawn on the overlay, centering it on the flight line.

With the aid of the geologists, Pisgah Crater was divided into 14 areas by geologic composition. The geologic names of the areas are listed in Table I. It should be noted that the areas were divided by geologic composition, not necessarily by textures or radar scattering properties. The areas were numbered 1 through 14 for reference purposes.

The time at the center of the photographs had been previously determined from the clock printed on each photo. The time at the edges of each geologic area could be determined by interpolation.

Since information had been received that the time on the Return vs. Angle graphs did not correspond exactly to the time imprinted on the aerial photos, the time offset had to be determined. The Return vs. Angle curves were examined to find a prominent change in curve shape. A prominent change occurred at 15-06-57, 20 "graph time," which was assumed to correspond to the leading edge of area 14 on the photos. The difference between "graph time" and "photo time" was determined to be 37.7 seconds, which agreed with the approximate known difference.

Since the photo times at the boundaries of the 14 areas were known, the corresponding graph times could be determined by adding 37.7 seconds to the photo times. At this point, the 135 graphs, with two Return vs. Angle curves per graph, could be separated into 14 groups corresponding to the 14 areas on the photographs. Obviously erroneous curves at the beginning and end of the flight were not included in the processing.

The first step in the actual data processing was to determine an average curve for each of the 14 areas. The magnitude of the return for each angle was read from the forebeam curves and was tabulated by area. Then the magnitudes were added for each angle and the total was divided by the number of readings to obtain an average value for that angle in the area. An average Return vs. Angle curve could then be plotted for each area, as shown in Figure 2. This display illustrates the variation of the Return vs. Angle curves of the different geological areas of Pisgah Crater.

Next the magnitudes of each of the angles on the 14 average curves were added and divided by 14 to produce an Overall Average Curve for the entire flight. For each area the magnitude of the average angle readings were subtracted from the corresponding magnitudes on the Overall Average Curve. This produced 14 curves displaying deviation of the area curve from the Overall Average Curve. The Deviation from Average curves are displayed in Figure 3, with corresponding ground areas indicated.

The tabulated data was given to computer personnel to be processed by a Principal Components Analysis program. This program is intended to indicate which three angles, of the eight possible, contain the most information about the terrain being examined. The forebeam data will be processed first to provide a Principal Components Analysis. The analysis will be checked by processing aftbeam data.

The aftbeam data was processed in the same manner as the forebeam. The graphs were divided into 14 groups corresponding to the 14 ground areas, the magnitude of the return for each angle was read from the graphs and tabulated. Average curves were determined and were plotted on the corresponding average curve from the forebeam data. By visual inspection the two curves appeared to agree well, except at the  $60^{\circ}$  values. Also, the average curves for Area 13 did not correspond well, however only a few data points

were present for this area, and disagreement was not surprising.

The Bermuda Ocean flight data was not processed. After examination of the graphs and Sea State spectral density curves, no prominent variations were noticed and no justification for the large amount of hand labor required for processing was seen. This data may be processed at a later date when computer processing can be used.

## V. Presentation of Data

One of the problems inherent in the Ryan Scatterometry system is the presentation of the data in a method which is easily understood, and which can emphasize minor changes in the terrain return. The Return vs. Angle curves contain this information, however an easily understood presentation method is desirable. Several possible presentation methods are shown by Dr. Moore in CRES Report No. 61-11.

The first presentation methods used were as previously discussed and shown in Figures 2 and 3. The Return vs. Angle curves and Deviation from Average Curves were plotted along a small photo of Pisgah Crater, with arrows designating the correspondence between curves and areas. This is the most straightforward and simplest method of data presentation, however the changes in curve shape may not have obvious meaning to an observer, and small changes in curve shape are not prominent.

Following presentation methods attempted to present information from the Deviation from Average Curves. The Deviation from Average Curves better illustrated curve variation than the Return vs. Angle curves, and presented a more useable range of magnitudes. By visual inspection the  $5^{\circ}$ ,  $30^{\circ}$  and  $60^{\circ}$  values from the Deviation from Average curves were chosen as providing the three best points to characterize the curve shape.

Colored bar presentations were considered next as shown in Figure 4. Any presentation involving length of a bar appears to have the inherent difficulty that if the Deviation from Average value is small, the length of the bar approaches zero. If the bar length is small, color and angle information become difficult to read. This problem could probably



be overcome by defining a minimum length as equal to zero deviation, or by using a nonlinear scale. The methods illustrated in Figure 4b and 4c were used for all 14 areas. The method in 4b dramatically illustrated changes in Deviation from Average values for each of the three angles, however the presentation had a confusing appearance. The method in Figure 4c was easy to read, but doesn't appear to offer any advantage over the display of Deviation from Average curves themselves.

The next presentation method attempted a color-hue, bar-height combination as shown in Figure 5. The following procedure was used to determine the color hue: The Deviation from Average values were tabulated for the  $5^\circ$ ,  $30^\circ$  and  $60^\circ$  values. Five db was added to each value to obtain all positive values. The  $5^\circ$  and  $30^\circ$  values were normalized to give x and y coordinates on the standard CIE Chromaticity Diagram, as shown in Figure 6. The vertical height of the color bar was used to represent the positive or negative value of the  $60^\circ$  Deviation from Average. (The five db addition was not used in determining the bar vertical height; both positive and negative values were permitted.) The horizontal lengths of the color bars corresponded to area lengths on the aerial photographs. This method had the advantage of definitely specifying a color hue; an identical hue could be reproduced anywhere by knowledge of the coordinates on the CIE Chromaticity Diagram. Possible difficulties would include technical difficulty with producing a color hue from the coordinates, and the fact that certain coordinate values produced by normalizing may lie completely outside the color "triangle" and could not be represented by any color. Also the different bar heights were confusing, although two parameter values would completely specify the color, and some method was needed to include the third angle.

The final presentation method attempted was the combination of the  $5^\circ$ ,  $30^\circ$  and  $60^\circ$  values into a single color representing the characteristics of a certain ground area. The results are shown in Figure 7. The colors were produced by overlapping three colored beams from three slide projectors onto a screen. The first projector had a Kodak Wratten Filter #29 (Red)

in front of the lense, and by the use of a variac to change the projection lamp voltage, the intensity of the projected red light represented the 5° Deviation from Average value. In a similar manner, a projector with a #47A blue filter represented the 30° value and a projector with a #61 green filter represented the 60° value. The tabulated Deviation from Average values were normalized to obtain percentages. As before, five db was added to all values to obtain positive percentages.

$$5^{\circ} \text{ percentage} = \text{Red} = \frac{5^{\circ} \text{ value}}{5^{\circ} \text{ value} + 30^{\circ} \text{ value} + 60^{\circ} \text{ value}}$$

$$30^{\circ} \text{ percentage} = \text{Blue} = \frac{30^{\circ} \text{ value}}{5^{\circ} \text{ value} + 30^{\circ} \text{ value} + 60^{\circ} \text{ value}}$$

$$60^{\circ} \text{ percentage} = \text{Green} = \frac{60^{\circ} \text{ value}}{5^{\circ} \text{ value} + 30^{\circ} \text{ value} + 60^{\circ} \text{ value}}$$

As a first test and for the simplest method, it was noted the projector rheostat scales were numbered from zero to 100, and that a setting of 20 resulted in the bulb being completely dark, and a setting of 100 gave full brightness. The percentage figures were placed on the rheostats according to Table 2 in Figure 8. The three projector beams overlapped, as shown, giving a color combination which represented the three Deviation from Average values, and hopefully also represented certain characteristics of the ground area.

The 5°, 30° and 60° percentages for each of the 14 areas were placed in sequence on the projector rheostats and the resulting color combinations were photographed. Color prints were made, and the color "chips" used in Figure 7 were cut from the prints.

This method was the simplest, fastest and produced the most dynamic range of colors of any method attempted. However it was not a

quantitative method since projector brilliance was not a linear function of rheostat settings as assumed. Also the results from the same data may not be reproducible on any other equipment.

An unsuccessful attempt was made to develop a quantitative method to obtain the color combinations. The method used will be described briefly, for future reference. The x and y coordinates for each of the Kodak Wratten filters were located from a Kodak Data book and were plotted on the CIE Chromaticity Diagram as shown in Figure 9. It was then possible to calculate the percentage brilliance needed for each color so their combination would theoretically produce a pure white. The calculation method was the same as considering the color "triangle" as being a plane pivoted about the pure white point. The percentage of each color was considered as a weight, and the "triangle" was balanced about the Pure White point by computing moments in the x and y directions. The calculations indicated 26.8% Red plus 44.6% Blue plus 28.5% Green should produce a pure white, using these Kodak filters. A Gossen cadmium sulfide photographic lightmeter indicated the maximum BLUE intensity was eight foot candles, the lowest maximum intensity of the three colors. Therefore eight footcandles was taken as equalling 44.6%, giving 4.8 footcandles = 26.8% for RED and 5.1 footcandles = 28.5% for GREEN. The lightmeter was used to individually set the projectors at their calculated brilliance and the three beams were combined. The result appeared bluish but perhaps will appear white on photographic film. It was later discovered the lightmeter does not have equal response to all colors, and therefore caused some inaccuracy.

Next the lightmeter was used to obtain a percentage brilliance vs. voltage curve for each projector and its filter. The Deviation from Average percentage values were then converted into corresponding projector voltages by use of these curves. Color combinations were attempted by using the voltage figures corresponding to a certain area. However the resulting combinations were pastel shades very close to white, and a satisfactory range of colors was not produced by this method.

**VI. Later Improvements**

After discussion of the color "chips" in part V 7 with geology personnel, the Pisgah Crater area was further subdivided into 21 areas. These areas are believed to have different radar returns. The Return vs. Angle curves will be summed and averaged for these areas as before and the results used to produce color chips.

TABLE I GEOLOGIC NAMES OF AREAS

Area 1	Alluvial material
Area 2	Porphyritic olivine basalt flows of second eruptive phase plus windblown alluvial material
Area 3	Alluvial material
Area 4	Microporphyritic olivine basalt flows of first eruptive phase
Area 5	Cinder cone
Area 6	Porphyritic olivine basalt flows of final eruptive phase
Area 7	Porphyritic olivine basalt flows of second eruptive phase
Area 8	Porphyritic olivine basalt flows of secondary eruptive phase, faulted area
Area 9	Porphyritic olivine basalt flows of second eruptive phase
Area 10	Porphyritic olivine basalt flows of final eruptive phase
Area 11	Porphyritic olivine basalt flows of second eruptive phase
Area 12	Microporphyritic olivine basalt flows of first eruptive phase
Area 13	Lake sediments and basalt
Area 14	Playa Lake sediment

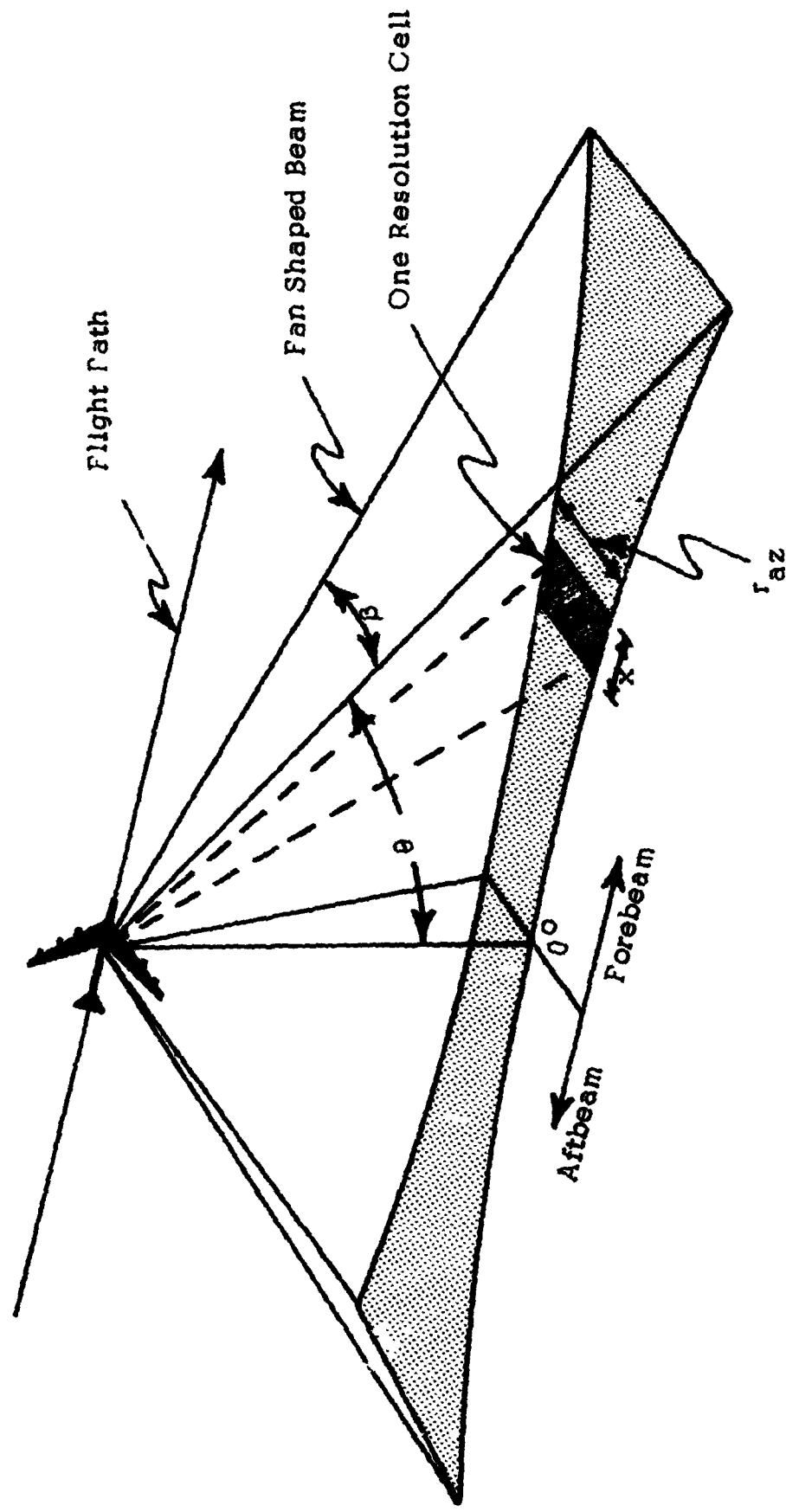


Figure 1

RYAN SCATTEROMETER SYSTEM



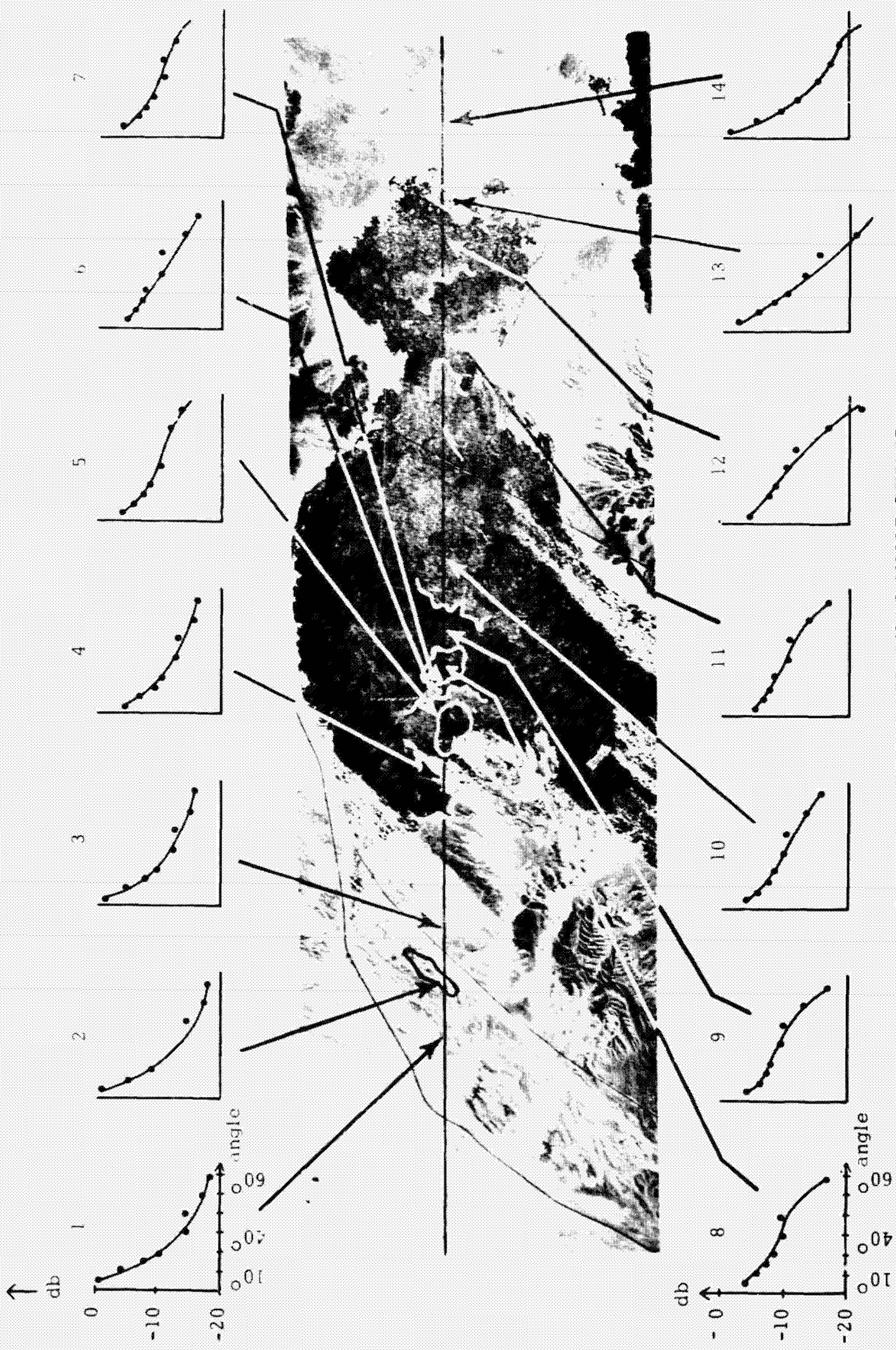


Figure 2. AVERAGE RETURN VS ANGLE CURVES



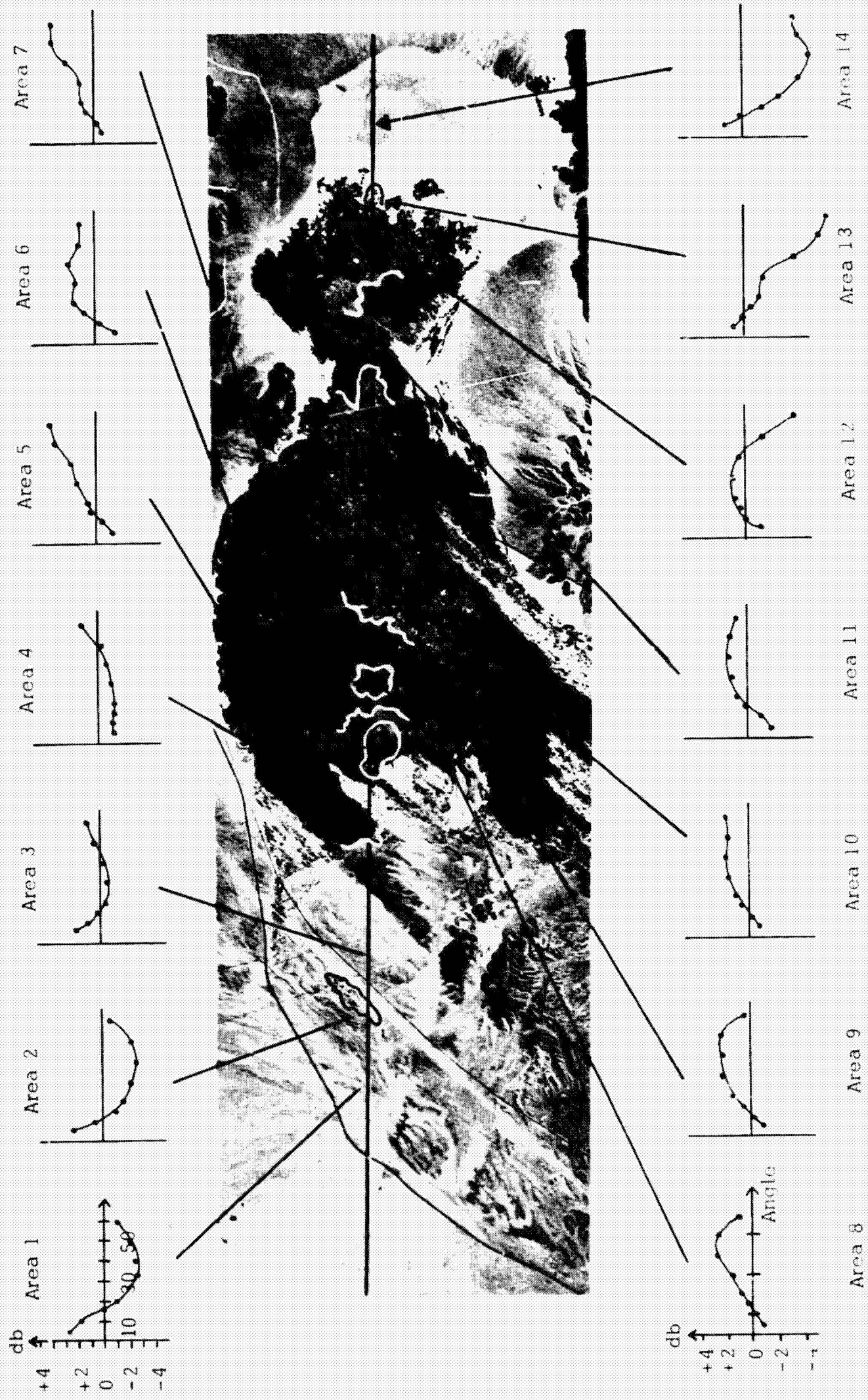
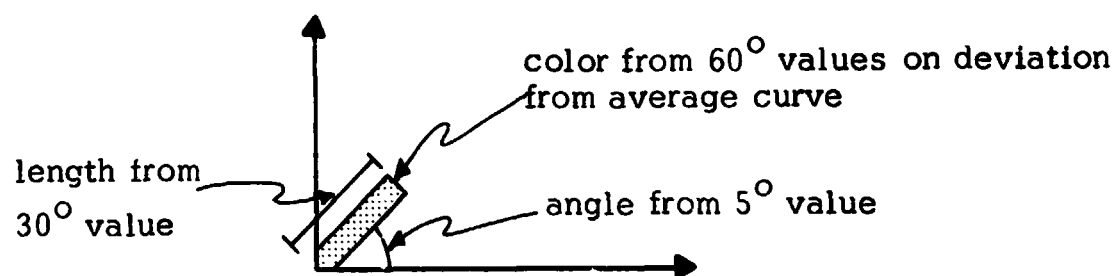
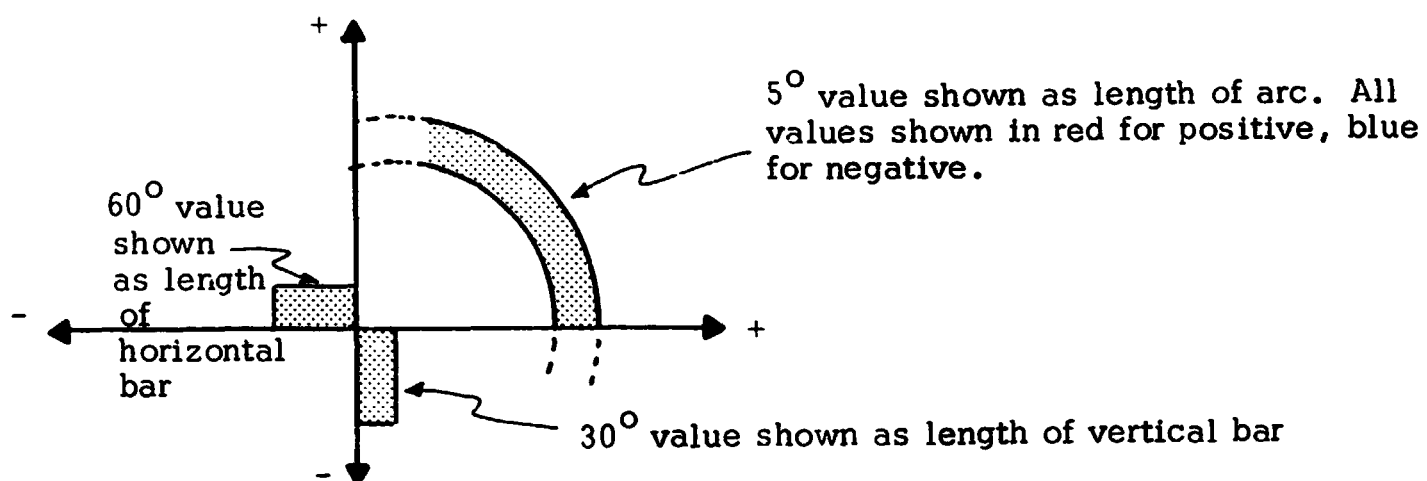


Figure 3. DEVIATION FROM AVERAGE CURVES

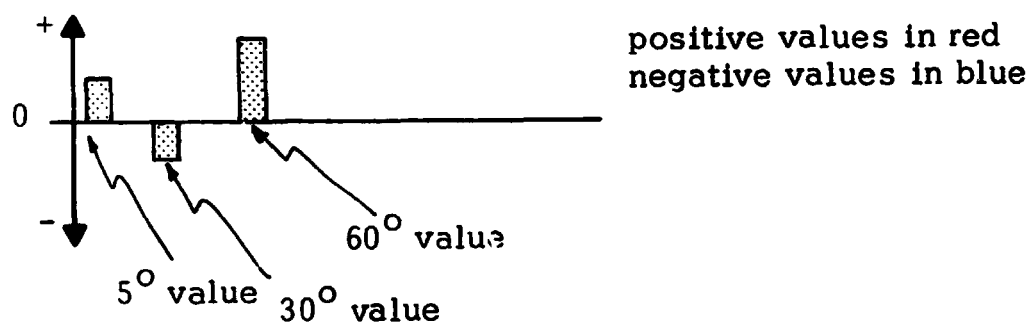




a) Angle-Color-Length Presentation



b) Arc-Horizontal Bar-Vertical Bar-Two Color Presentation



c) Bar-Two Color Presentation

Figure 4

POSSIBLE PRESENTATION METHODS

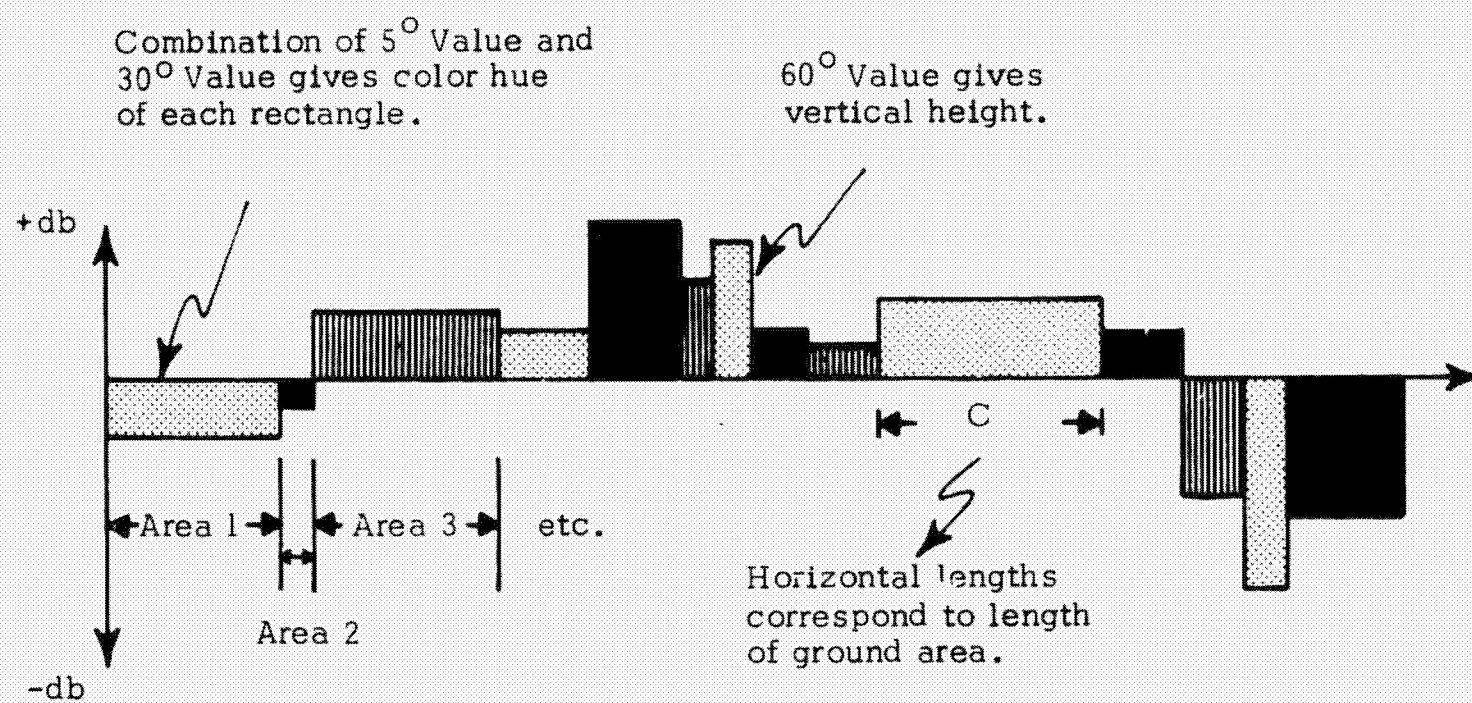
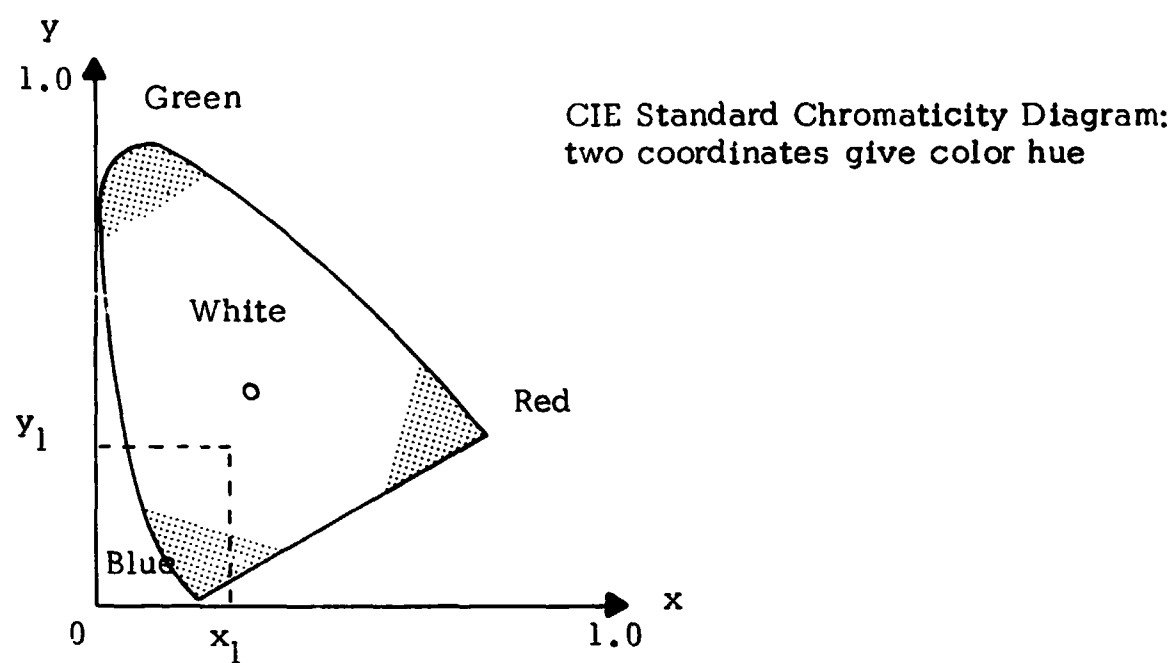


Figure 5

COLOR HUE-BAR HEIGHT PRESENTATION



Conversion of deviation from average values into coordinates

$$x \text{ coordinate} = \frac{5^{\circ} \text{ value}}{5^{\circ} \text{ value} + 30^{\circ} \text{ value} + 60^{\circ} \text{ value}}$$

$$y \text{ coordinate} = \frac{30^{\circ} \text{ value}}{5^{\circ} \text{ value} + 30^{\circ} \text{ value} + 60^{\circ} \text{ value}}$$

Figure 6

STANDARD CIE CHROMATICITY DIAGRAM

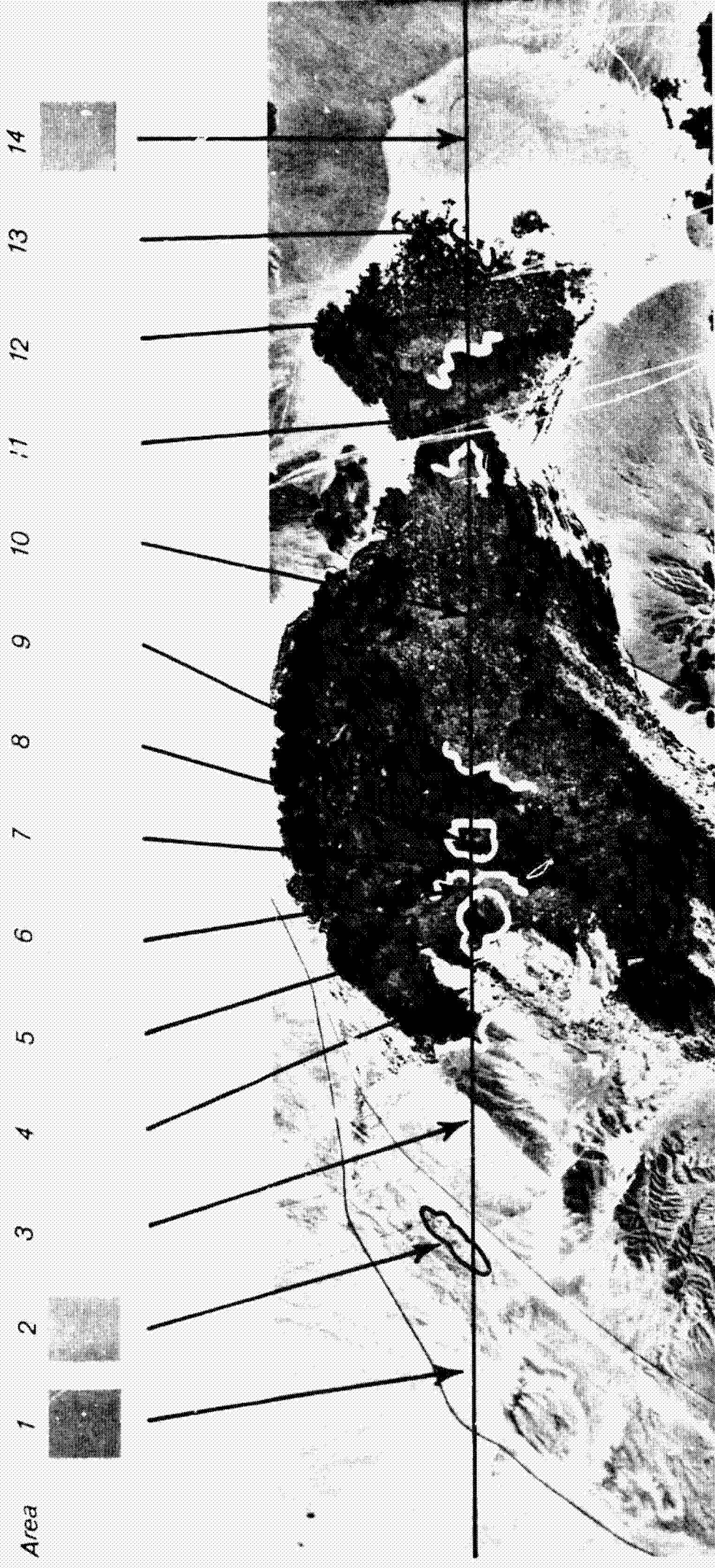


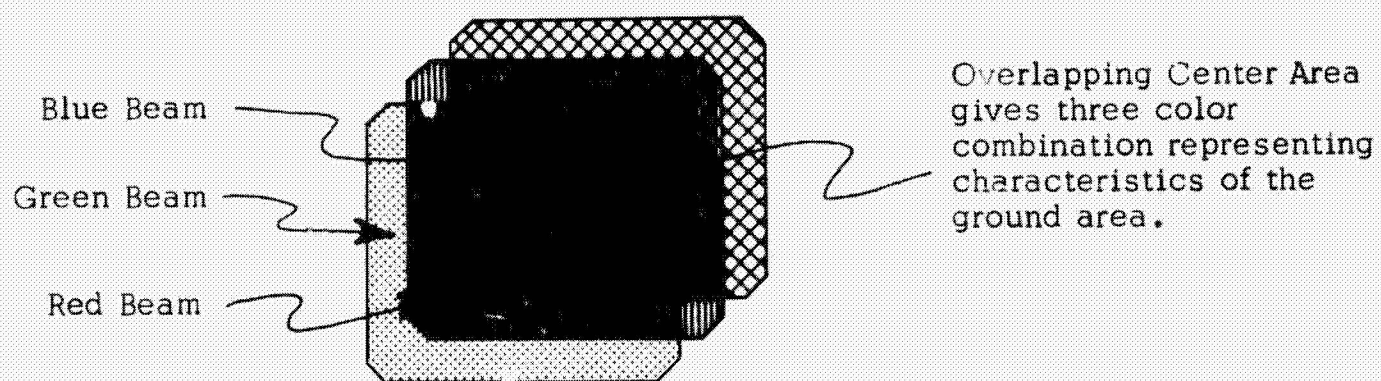
Figure 7. THREE COLOR COMBINATION PRESENTATION



Table 2  
Conversion of Percentage Values to Rheostat Settings

<u>Angle Percentage Values</u>	<u>Projector Rheostat Settings</u>	<u>Apparent Projector Brilliance</u>
0%	20	0%
25%	40	25%
50%	60	50%
75%	80	75%
100%	100	100%

Overlapping Color Beams



Projector Setup for Three Color Combination

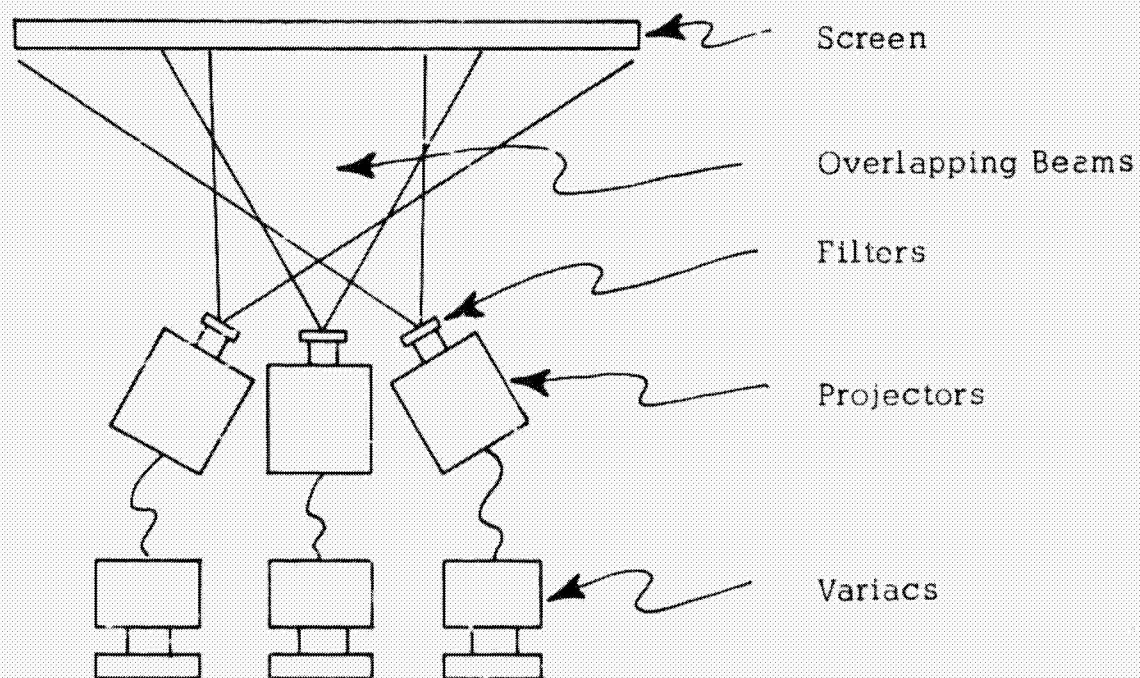


Figure 8.

THREE COLOR COMBINATION METHOD

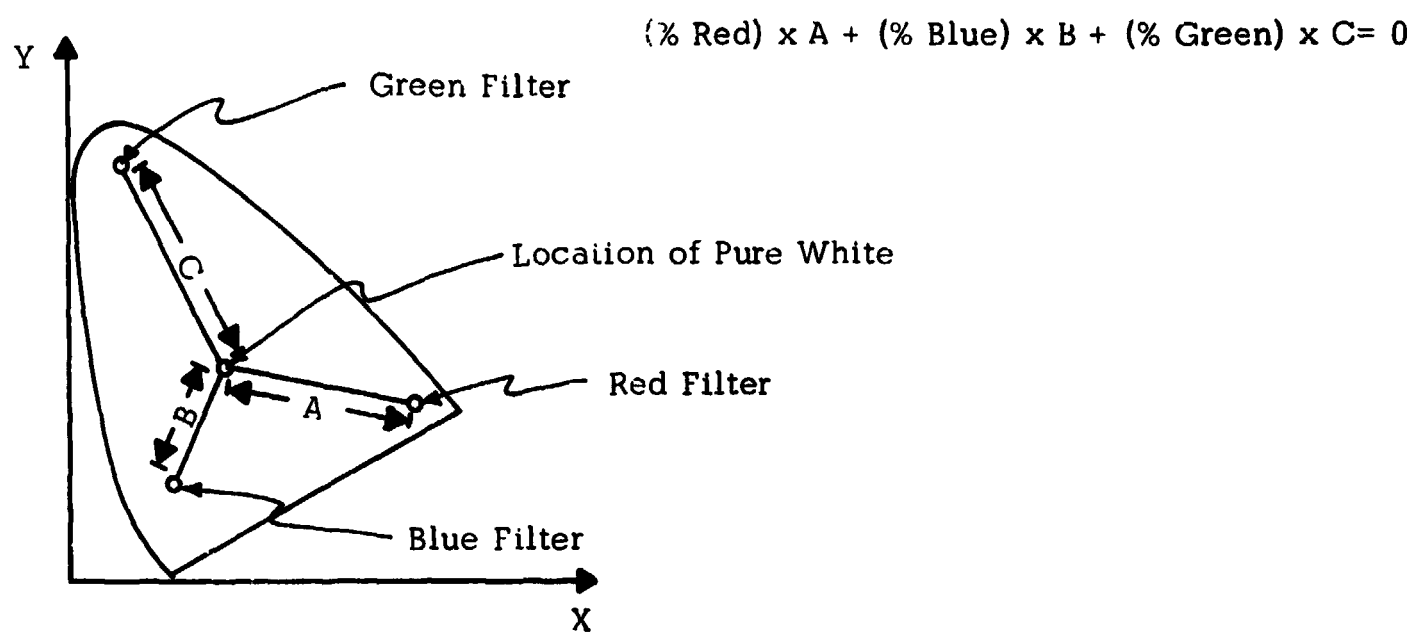


Figure 9.

CALCULATION OF COLOR PERCENTAGES TO OBTAIN PURE WHITE